UNIVERSITÉ DE GENÈVE

Archive ouverte UNIGE
https://archive-ouverte.unige.ch

Rapport technique | 2013 | Open Access

This version of the publication is provided by the author(s) and made available in accordance with the copyright holder(s).

Solar radiation resource in Geneva: measurements, modeling, data quality control, format and accessibility

Ineichen, Pierre

How to cite

INEICHEN, Pierre. Solar radiation resource in Geneva: measurements, modeling, data quality control, format and accessibility. 2013

This publication URL: https://archive-ouverte.unige.ch//unige:29599

© This document is protected by copyright. Please refer to copyright holder(s) for terms of use.

UNIVERSITÉ
DE GENÈVE

INSTITUT DES SCIENCES
DE L'ENVIRONNEMENT

Solar radiation resource in Geneva: measurements, modeling, data quality control, format and accessibility

Pierre Ineichen
University of Geneva
September 2013

Solar radiation resource in Geneva: measurements, modeling, data quality control, format and accessibility

Pierre Ineichen
University of Geneva
September 2013

Abstract

Solar radiation parameters are acquired in the region of Geneva since several tens of years in order to assess the local solar resource. The acquisition support, the number and type of the acquired parameters and the sites of measurements changed several times during these decades.

Nowadays, two sites are maintained by the Energy Group of the Institute of Environmental Sciences, and a third station by the Architecture High School. The data are displayed in real time on the World Wide Web and the archived data are freely accessible through ascii files (www.unige.ch/energie).

The data are used in several fields for model development and validation, solar power plants simulation, heating and cooling system study, new technologies development, etc.

The present report describes the sites, the sensors, the sensors calibration method, the data display and their accessibility.

1. Introduction

The Energy Group of the Institute for Environmental Sciences (ISE) of the University of Geneva (UniGE), former Centre Universitaire d'Etude des Problèmes de l'Energie (CUEPE), is active in the field of solar radiation measurements and modeling since several tens of years. Indeed, the first continuous acquisition of solar radiation data was implemented in 1978 in the city of Geneva on the roof of a university building. In 1991, the acquisition system was moved to a nearby higher building at «La Jonction». In 2010, we had to move again the acquisition system to the Battelle Campus, in the periphery of Geneva, in Carouge. In parallel, two other sites were equiped, one in Bernex, and another within the city at the Architecture highschool (hépia).

These long term solar radiation measurements are an essential support to solar ressource modeling. The following studies represent an non-exhaustive list of work done on the basis of the long term measurements acquired in Geneva:

- diffuse irradiance acquired with different methods were used to study the corrective factor involved in these measurements [Ineichen et al. 1984, Ineichen et al. 1990]
- modeling of the downwards infrared radiation, correlation with the total irradiance [Ineichen et al. 1984]
- modeling the UVB radiation in correlation with the global and beam irradiances [Baudry et al. 1996]
- measurements and analysis of the reflected radiation on inclined and oriented surfaces, importance of its correct determination [Ineichen et al. 1987]
- luminous efficacy modeling and validation applied on architecture projects [Molineaux et al. 1995, Perez et al. 1990]
- sky luminance distribution modeling [Ineichen et al. 1994, Perez et al. 1993]
- evaluating the beam component from the knowledge of the solely global irradiance [Perez et al. 1992, Ineichen 2008]
- transposition of the irradiance from horizontal to oriented and tilted surfaces [Perez et al. 1987, Ineichen et al. 1988, Ineichen 2011]
- analysis, validation and modeling of the clear sky radiation [Ineichen 2006, Ineichen 2008]
- turbidity and aerosol quantification [Ineichen 2008, Ineichen 2010]
- long term satellite derived irradiance modelization and validation [Ineichen et al. 1999, 2000, 2009, Ineichen 2011, 2013, Perez et al. 2002]

2. Measurements sites

The first measurements were initiated in 1978 in the city of Geneva, with only a few parameters. Year after year, we moved the sites, changed the sensors to higher

quality, added parameters and locations of acquisition.

2.1 Location and parameters

The first acquisition site was situated on the roof of an university buidling near of the center of the city of Geneva (latitude: 46.198°N, longitude: 6.133°E, altitude: 390m).

The acquisition system was a graphical recorder, taking a instantaneous measurement every 15 minutes. The global irradiance on a horizontal plane, the shading ring horizontal diffuse irradiance and the ambient temperature were acquired. In 1979, the four (north, east, south and west) vertical global irradiances, the 45° south oriented global irradiance, the wet bulb temperature, the wind velocity and the infrared sky radiation were added the system. In 1981, a shading disk was installed for the measurement of the diffuse component.

In addition to this acquisition system, two years of measurements were done in the countryside, in Sauverny (latitude: 46.308°N, longitude: 6.134°E, altitude: 475m), were the global and diffuse irradiances, dry and wet bulb temperatures, and infrared sky radiation were acquired.

During the years 1986-1987, we changed all the K+Z CM5 pyranometers by K+Z CM10 and new parameters were included in the acquisition list. They concern the global on south-facing planes inclined at 30° and 60°. In addition, all the measurement planes were fitted with artificial horizons preventing the radiation reflected by the ground from reaching the measuring cell. The reflected radiation was measured by other instruments on the same planes. The direct radiation was acquired by a normal incident pyrheliometer (Eppley NIP) to make it possible to precisely determine the diffuse radiation on all the planes. All the measuring instruments were Kipp & Zonen CM 10 thermopile pyranometers.

In 1991, we moved the system to a nearby 15 floors building (latitude: 46.199°N, longitude: 6.131°E, altitude: 420m), and added daylight sensors. We then removed the measurements on tilted and oriented planes, as well as the infrared sensor. This site was active until 2010.

In 2010, the site of measurements was moved to Carouge, on the Battelle campus (latitude: 46.176°N, longitude: 6.139°E, altitude: 432m). In addition, two other sites were implemented in the city and in the countryside, respectively at the Architecture high school (latitude: 46.210°N, longitude: 6.135°E, altitude: 420m) and in Bernex (latitude: 46.172°N, longitude: 6.067°E, altitude: 473m).

The acquired parameters in the different sites are given in Table I.

2.2 Horizons

The horizon profile knowledge of the acquisition sites is important for the interpretation and the use of the data. Indeed, the beam irradiance is blocked by the geographic and near horizon; this becomes important when dealing with east or west vertical surfaces. Even if the horizon should be as low as possible, the correct knowledge of it

Table I Acquisition site in Geneva: parameters and radiation instruments

	ScII				Sny	Jct	Bat	Ber	Pra
	1978 1979	1979 1980	1980 1982	1986 1987	1980 1981	1991 2010	2010	2010	2010
Horizontal global irradiance	CM5	CM5	CM5	CM10	CM6	CM10	CM10	CM10	CM10
Horizontal diffuse irradiance (shading ring)	CM5	CM5	CM5	CM10					CM10
Horizontal diffuse irradiance (shading disk)				CM10	CM5				
Horizontal diffuse irradiance (SPN1)								SPN1	
Normal beam irradiance				NIP		NIP	NIP	SPN2	
Vertical north		CM5	CM6	CM10					
Vertical east		CM5	CM6	CM10					
Vertical south		CM5	CM6	CM10					
Vertical wset		CM5	CM6	CM10					
South 45°		CM5	CM6	CM10					
South 30° and 60°				CM10					
Infrared sky radiation		PIR	PIR	PIR	PIR			PIR	
Ultraviolet UVB (1994)						YES			
Illuminances (horizontal and vertical, 91-95)						LiCor			
Luminance (145 solid angles, 1991-1994)						PRC			
Ambient temperature									
Wet bulb temperature									
Relative humidity									
Wind speed and direction									

Kipp + Zonen CM5 and CM10 pyranometers
Eppely Normal Incident Pyrheliometer (NIP)
Eppely infrared Pyrgeometer (PIR)

ScII University building
Sny Sauverny
Jct Jonction

Bat Battelle
Ber Bernex
Pra Prairie

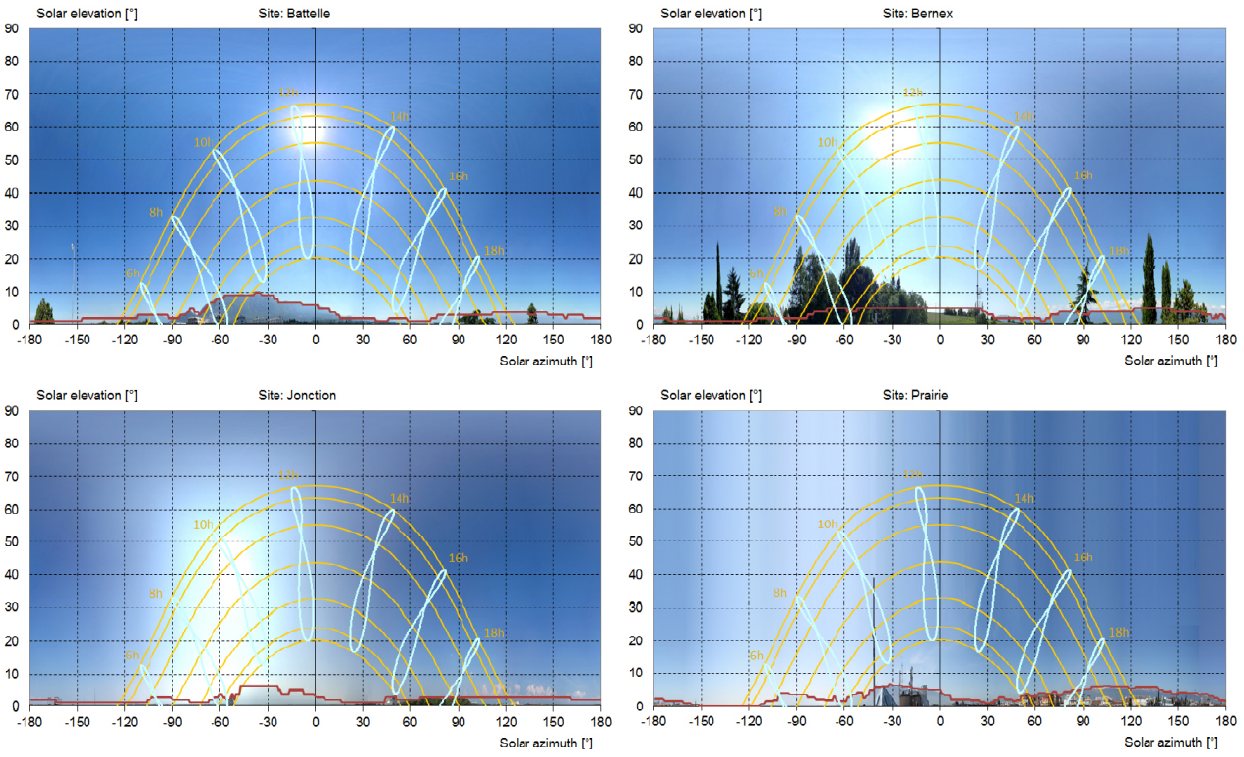

Figure 1 Near (image) and geographic (red line) horizons for the main acquisition sites in Geneva

permits the use of the data as input for validation or simulation with a good precision. Figure 1 represents the horizon of the four main acquisition sites. The backgroud image is what is seen by the sensors, whereas the red line represents the geographic horizon as retrieved from the Meteonorm software [www.meteonorm.com].

3. Calibration and quality control

Sensor calibration is the key point for precise acquisition in the field of solar radiation. The radiation sensors should be calibrated by comparison against a sub-standard before the beginning of the acquisition period, and then, if possible, every year. Due to possible errors and inaccuracies, a post-calibration is difficult to conduct.

The validity of the results obtained from the use of measured data is highly correlated with the quality of the data bank used as reference. Controlling data quality is therefore the first step to perform in the process of validating models against ground data. This essential step should be devised properly and automated in order to rapidly detect significant instrumental problems like sensor failure or errors in calibration, orientation, leveling, tracking, consistency, etc. A stringent control quality procedure must therefore be adopted, and its various elements are described in what follows.

If the three solar irradiance components—beam, diffuse and global—are available, a consistency test can be applied, based on the closure equation that link them.

An a posteriori automatic quality control cannot detect all acquisition problems that could have happened, however. The remaining elements to be assessed are threefold:

- the measurement's time stamp (needed to compute the solar geometry),
- the sensors' calibration coefficient used to convert the acquired data into physical values,
- the coherence between the parameters.

3.1 Time stamp

To detect a possible time shift in the data, the symmetry (with respect to solar noon) of the irradiance for very clear days is visually checked. The global horizontal and direct normal irradiances are plotted versus the sine of the solar elevation angle for specific clear days. If the time stamp is correct, the afternoon curve should normally lay over the morning curve as visualized in Figure 2. Exceptions do occur, however, at sites where the atmospheric turbidity changes during the day, due for example to topography-induced effects, where the clear-sky irradiance can be significantly different in the afternoon than in the morning. As the global irradiance is less sensitive to turbidity, the accordance morning/afternoon is of more importance for the global component.

If this test is positive, a verification can be done on the whole time series with the help of the global clearness indices K_t and K_b defined respectively as:

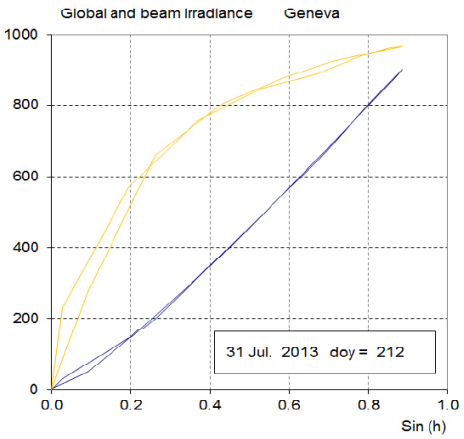

Figure 2 (above) G_h and B_n represented versus the sinus of the solar elevation angle for a clear day, July 2013.

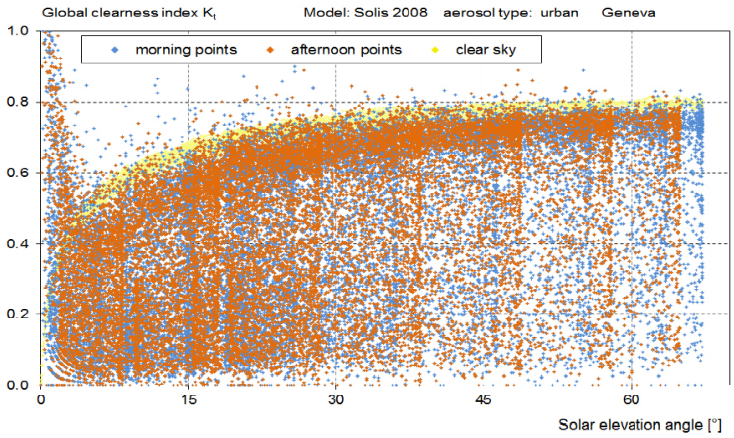

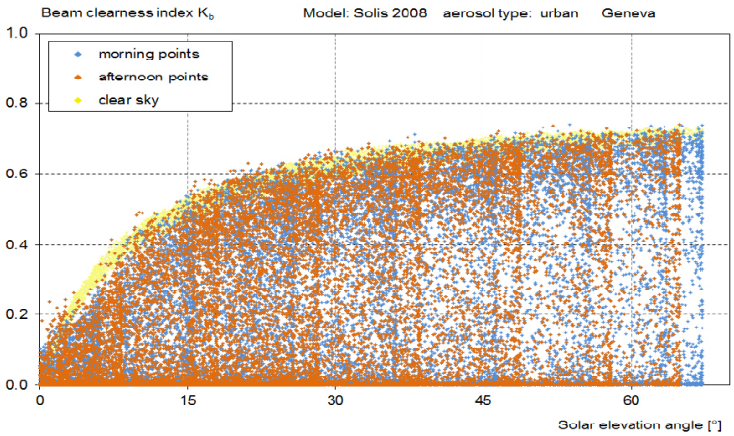

Figure 3 (right) K_t and K_b represented separately for the morning (blue) and the afternoon (red) data, versus the solar elevation angle for eight years of hourly values.

Corresponding clear sky model data are represented in light yellow.

$$K_t = \frac{G_h}{I_o \cdot \sin(h)} \qquad K_b = \frac{B_n}{I_o}$$

where G_h is the global horizontal irradiance, B_n the normal beam irradiance, I_o is the extraterrestrial irradiance (i.e., the solar constant corrected for the actual sun-earth distance), and h the solar elevation angle. The clearness index is then plotted for the morning and afternoon data separately, e.g. using different colors. The upper limit, representative of clear-sky conditions, should lay over for the morning and the afternoon data as represented on Figure 3 for eight years of global irradiance data. Ideal hourly clear-sky values, calculated with the solis clear sky model [Ineichen 2008], are plotted in light yellow on the same graph. This test is very sensitive since a time shift of only a few minutes will conduct to a visible asymmetry.

When these two conditions (symmetry around solar noon and consistency of envelope) are fulfilled, the time stamp of the data bank can be considered correct, and the solar geometry can be precisely calculated.

3.2 Sensor calibration

The sensor calibration should be done regularly against a sub-standard which is not used for continuous acquisition. The sub-standard is a reference instrument, of the same type than the routine acquisition instruments; it is regularly either sent to a national metrology institute, or calibrated against a absolute instrument.

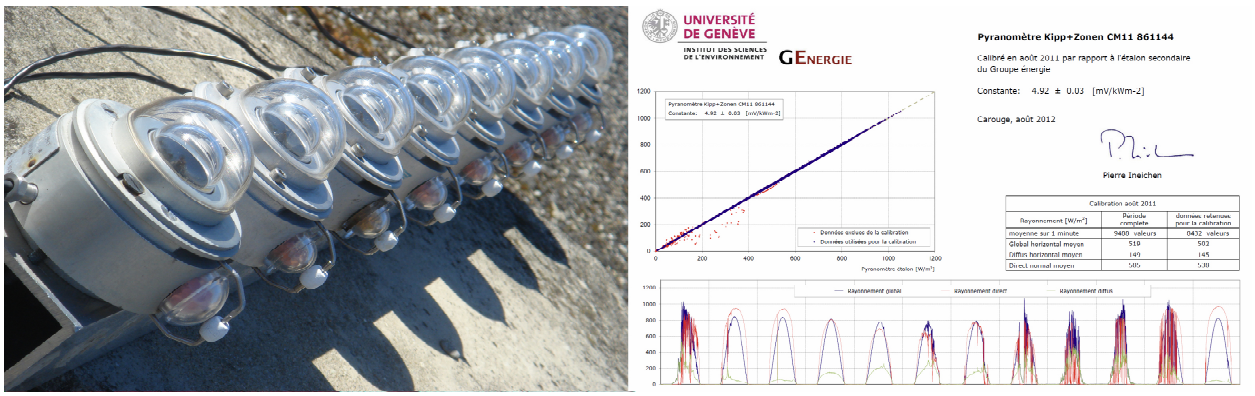

Figure 4 Kipp+Zonen CM10 during calibration (left) and resulting certificat (right)

In the first year of our activity, we sent every couple of years our sub-standard to the World Radiometric Center (WRC) in Davos for calibration. Then we bought an absolute cavity radiometer PMO 6 from the WRC in order to conduct ourself a local calibration of the sub-standard.

The routine used instruments are then regularly calibrated against the sub-standard during a 10 days period, if possible covering all type of meteorological conditions and solar elevation angles (i.e. preferably in summer). During this period of calibration, only values acquired during stable conditions are kept, the measurements are minute averages. An illustration of the obtained calibration results is given on Figure 4.

Depending on the acquisition situation, it is not always easy or possible to calibrate the sensor during the measurements. The sensors' calibration can then be verified for clear sky conditions by comparison against data from a nearby station or by a long term comparison.

To conduct this test, for each day, the highest hourly value of G_h and B_n is selected from the measurements and plotted against the day of the year as illustrated in Figure 5 where the site of Battelle and Bernex are compared. These points are representative of the clearest daily conditions. As the highest value for each day is selected, the upper limit normally represents clear-sky conditions (for G_h, it happens that higher-than-clear-sky values are obtained under partly cloudy (scattered clouds), high-sun conditions, this is why this test should not be applied for data with time

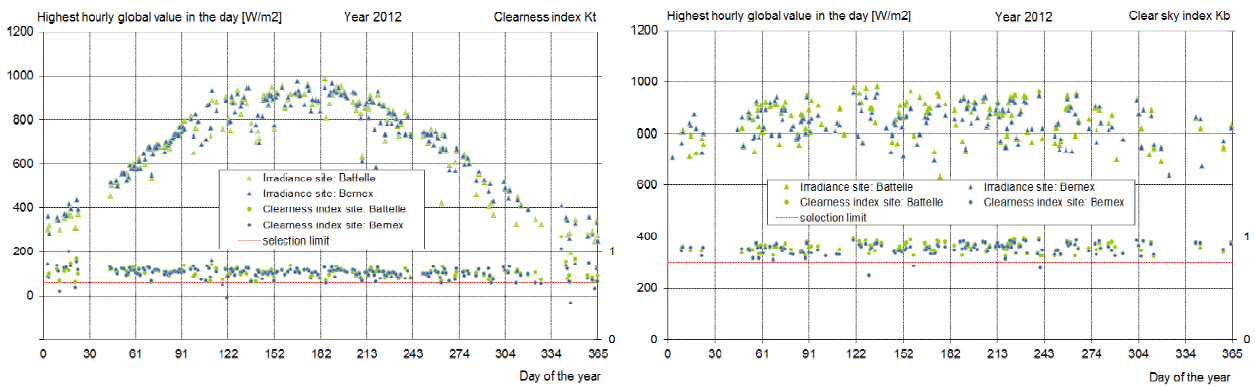

Figure 5 Comparison of the daily highest value of respectively the global and the beam irradiances reported versus the day of the year for the two sites. The corresponding modified clearness index and clear sky index are also represented.

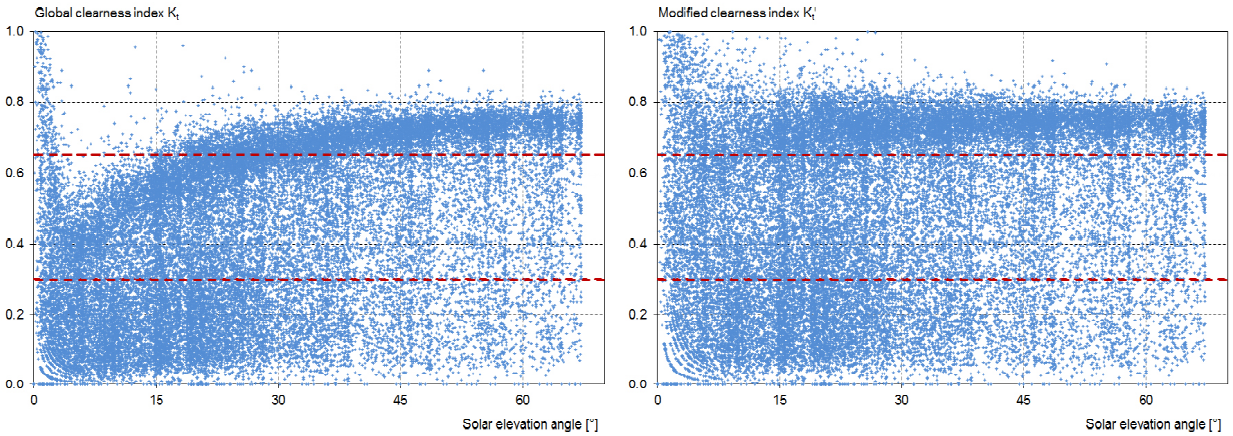

Figure 6 Global clearness index and modified clearness index versus the solar elevation angle.

granularity lower than one hour). On such graphs, data from nearby sites, or from different years for the same site can be compared.

These graphs can be augmented by superimposing the modified clearness index K_t', which was defined by Perez et al. [1990] as:

$$K_t' = \frac{K_t}{(1.031 \cdot \exp(-1.4 / (0.9 + 9.4 / AM)) + 0.1)}$$

where *AM* is the optical air mass as defined by Kasten [1980]. This modified clearness index has the advantage of being relatively more independent from the solar elevation angle than K_t as illustrated on Figure 6.

This modified global clearness index is also used to delineate three K_t' zones to characterize the sky condition [Ineichen 2009]:

clear-sky conditions	$0.65 < K_t' \leq 1.00$
intermediate sky conditions	$0.30 < K_t' \leq 0.65$
cloudy sky conditions	$0.00 < K_t' \leq 0.30$

In the upper part of Figure 5, only values with $K_t' > 0.65$ are represented.

For B_n, the clear-sky index is defined as:

$$K_{bc} = \frac{B_n}{I_o \, e^{-MA \cdot (\delta_{cda} + \delta_w)}}$$

where δ_{cda} is the broadband clean and dry atmosphere optical depth, and δ_w is the water vapor optical depth. These two broadband optical depths can be evaluated following Molineaux et al. [1998] with simplified expressions:

$$\delta_{cda} = -0.101 + 0.235 \cdot MA^{-0.16} \qquad \delta_w = 0.112 \cdot MA^{-0.55} \cdot w^{0.34}$$

The denominator of K_{bc} is representative of the beam irradiance transmitted by a clean atmosphere. K_{bc} is represented on the right graph of Figure 4. On the upper part, only values for K_{bc} higher than 0.8 are represented.

The long term stability of the calibration can also be assessed with this method by

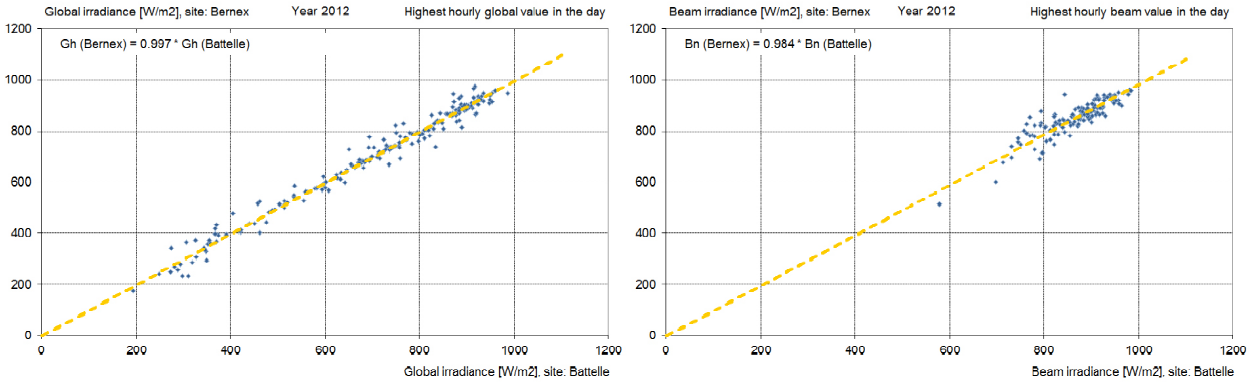

Figure 7 Scatter plots of the two data sets for the highest daily global and the beam hourly value. The slope given on the graph is representative of the calibration coefficient difference.

plotting on the same graph several years of data.

To quantitatively assess the correctness of the calibration factor, a linear regression is applied on the clearest hourly values selected for each day, between the two sets to be compared. This is illustrated in Figure 7 for the two components. The slope of the regression line is also shown for each case. This test is based on the assumption that the two sites are not too far one from the other with similar sunning, aerosol and water vapor atmospheric load conditions.

The same method can be used to assess the stability of the sensors' calibration. In this case, the irradiance components are compared year by year for the same site. Here again, the upper boundary should not change from one year to the other, if there are no significant changes in the turbidity and/or the humidity.

3.3 Components consistency

The consistency test between the G_h and B_n components can be verified with the help of the global and beam clearness indices.

The hourly beam clearness index is plotted versus the corresponding global index as illustrated on Figure 8. On the same graph, the clear-sky predictions from the Solis radiative model are represented for four different a priori values of *aod*. The

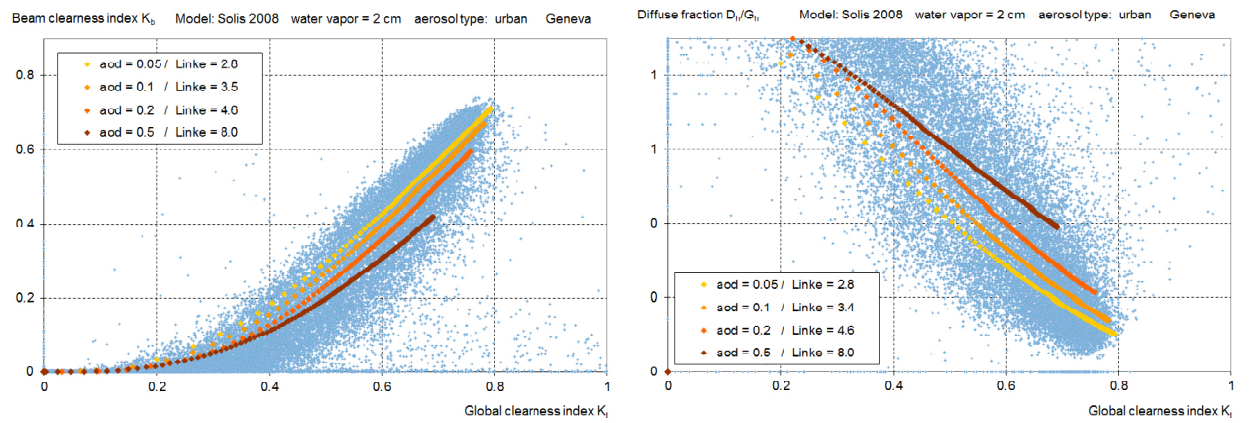

Figure 8 The beam clearness index (left) and the diffuse fraction (right) are plotted against the global clearness index. On the same graph, clear sky modelled values are represented for 4 different aerosol loads. The corresponding Linke turbidity coefficients are also indicated

corresponding Linke turbidity coefficient T_{Lam2} is then calculated from the B_n thus obtained:

$$B_n = I_o \, e^{(-\delta_{cda} \cdot T_{Lam2} \cdot MA)}$$

T_{Lam2} is evaluated for $AM = 2$ and its correspondence with *aod* is also indicated on the graph. Any important deviation between the predicted and measured clear-sky values indicates calibration uncertainties, pyrheliometer misalignement, soiled or shaded sensors, or miss-categorization of clear-sky conditions.

A similar test can be conducted with the diffuse fraction: on Figure 8 (right), it is represented against the global clearness index; it should lie in the same region than the clear sky model lines represented as above for different turbidity values.

4. Gap filling, aggregation and auxiliary data

As a data acquisition never works without breakdowns, and as the use of the data for simulation or TMY construction requires continuous time series, it is necessary to fill the possible gaps. After the gap filling step. the data can be aggregated into hourly, daily and monthly values. This is done by averaging and integration over the considered time period.

4.1 Gap filling

The gap filling is an essential step in the ground data time series acquisition process. Indeed, breakdown of the acquisition system is ineluctable and the gaps have to be filled in order to produce a continuous and complete time series.

In the Geneva region we maintain two data acquisition systems with a one minute time step, and one station with a ten minute time step. We use the following methods for the gap filling:

- in the case of one minute data acquisition breakdown, when available, the gap is filled with the data from the second acquisition site. The radiation and relative humidity data are kept without any changes, and the temperature data are shifted to avoid a step at the beginning and end of the gap. The gap filling is applied on the one minute time step data,
- in the ten minutes time series, the one minute data from the nearest site are aggregated in ten minutes,
- if the two one minute acquisition sites are broken down, the ten minutes data from the third site are aggregated in hourly values and used to fill the gap. This case never happened,
- when only the sun tracker is not working, the *aod* retrieved from one of the other site is used jointly with the local atmospheric water vapor content as input to the DirIndex model [Perez et al. 1992] for the evaluation of the beam component from the local global irradiance.

In the average, the maximum gap filling we applied on the data is less than 3% in term of time.

4.2 Data aggregation

All our data are aggregated into hourly, daily and monthly values in the following way:

- the ambient temperature, relative humidity, atmospheric pressure and wind speed are averaged over the time period,
- the wind direction is vectorially averaged,
- the global, beam and diffuse irradiances, and the infrared radiation are integrated over the time period,
- the corresponding time stamp in the data bank is set at the end of the time period, i.e. 14h is representative of data acquired from 13h to 14h.

4.3 Auxiliary data

From the measurements, a series of auxiliary data are calculated and added to the data bank. These are the following:

- from the ambient temperature and the relative humidity, the atmospheric water vapor content is evaluated with the use of Atwater model [Atwater 1976],
- the radiation received on an oriented and tilted surface is evaluated with the Perez transposition model [Perez et al. 1987], with a 20% albedo coefficient assumption,
- the sunshine duration is calculated from the normal beam irradiance, it is the time during which this irradiance exceeds a level of 120 [W/m^2].

5. Data access and file format

Our data are free and easily accessible through the internet in different forms: real time digital and graphical data, graphical archives, and archive ascii files in hourly, daily and monthly values [www.unige.ch/energie].

The format of the data files is a simple ascii, fixed length, comma separated format. Each file has header lines beginning with a # and describing the file content. A example is given on Figure 9.

The real time data are displayed for the three sites in four different windows: main windows with the digital data, and three daughter pages with respectively the solar radiation, the infrared radiation, temperature and relative humidity, and the wind and atmospheric pressure. Figure 10 illustrates the main window.

The graphical archives are weekly pages where all the parameters are displayed: the irradiances, temperature and relative humidity, atmospheric pressure, wind speed and direction, and irradiance evaluated on the four vertical planes. It is possible to navigate in the whole data bank.

```
#  Station             : Geneva (Battelle)     year      : 2013
#  Latitude            : 46.176ø N       Longitude:  6.139øE       altitude:  432m
#
#  doy                 : day of the year
#  time                : end of integration hour - UTC+1
#  lt                  : legal time used for geometry calculations - UTC+1
#  se   az             : solar elevation and azimuth at corresponding legal time
#  Gh   Dh   Bn        : global and diffuse on a horizontal plane and normal beam irradiances [Wh/m2h]
#                        diffuse irradiance calculated from the global and the beam irradiances
#  Ta   HR             : dry bulb temperature [øC] and relative humidity [%]
#  w                   : precipitable water content of the atmosphere [cm]
#  vv                  : wind speed [m/s]
#  dv                  : wind direction - from N=0ø   W=90ø   S=180ø   E=270ø
#  pr                  : atmospheric pressure at sea level [hp]
#
#  Tilted irradiances evaluated from the measured global and beam component with an albedo coefficient of 20%
#  Perez model: R. Perez et al. A new simplified version of the Perez diffuse irradiance model for tilted surfaces. Solar Energy 39 (1987)
#
# Gn   Ge   Gs   Gw      : global irradiance on a vertical plane - north - east - south and west [Wh/m2h]
# G35e   G35s   G35w    : global irradiance on a 35ø tilted plane - east - south and west [Wh/m2h]
#  G45s                : global irradiance on a 45ø tilted plane - south orientation [Wh/m2h]
#  G35_ 45             : global irradiance on a 35ø tilted and 45ø oriented plane (south=0) [Wh/m2h]
#  Gtrack              : global irradiance on a plane tracking the sun - perpendicular to the sun rays [Wh/m2h]
#  min sun             : sunshine duration in minutes (threshold on beam irradiance: 120 [W/m2]
#  IR                  : infrared radiation balance   [Wh/m2h]
#  IRd                 : incoming infrared radiation  [Wh/m2h]
#  IRup                : outgoing infrared radiation  [Wh/m2h]
#  missing data        : -99

#  copyright energy group (University of Geneva) 2013,  laste update:  09-09-2013  16:54:19
 doy, Io , time,    lt ,    se ,      az ,    Gh ,    Dh ,    Bn ,     Ta , HR ,     w  ,    vv , dv ,    pr    ,   Gn ,    Ge ,    Gs ,    Gw , G35e,   G35s,
   2, 1412,     9,    8.7,    2.6,    -52.3,     12,     12,      0,     1.9,   98,     1.0,    1.1, 182,   1021.7,     7,      3,      4,      7,     8,      9,
   2, 1412,    10,    9.5,    8.6,    -43.1,     83,     31,    280,     1.4,   98,     1.0,    0.9, 262,   1022.6,    24,    223,    262,     24,   187,    210,
   2, 1412,    11,   10.5,   14.8,    -30.5,    229,     39,    739,     2.5,   94,     1.0,    1.0, 294,   1023.3,    46,    439,    716,     46,   426,    585,
   2, 1412,    12,   11.5,   19.0,    -16.8,    305,     51,    783,     5.1,   84,     1.1,    1.0, 311,   1023.6,    59,    292,    831,     59,   400,    709,
   2, 1412,    13,   12.5,   20.7,     -2.2,    189,     74,    327,     5.9,   65,     0.9,    2.7,  50,   1023.3,    53,     91,    386,     53,   187,    356,
   2, 1412,    14,   13.5,   19.8,     12.4,    162,     87,    223,     6.0,   59,     0.8,    3.8,  62,   1023.2,    55,     55,    301,    110,   112,    285,
   2, 1412,    15,   14.5,   16.3,     26.5,     75,     65,     33,     5.9,   60,     0.9,    3.6,  43,   1023.8,    36,     36,     74,     52,    58,     89,
   2, 1412,    16,   15.5,   10.7,     39.4,    100,     53,    285,     5.9,   59,     0.8,    3.4,  55,   1024.3,    35,     35,    286,    257,    44,    234,
   2, 1412,    17,   16.4,    3.8,     50.5,     23,     19,     34,     5.7,   59,     0.8,    3.2,  35,   1024.9,    11,     11,     38,     39,    17,     36,
```

Figure 9 Data file format example

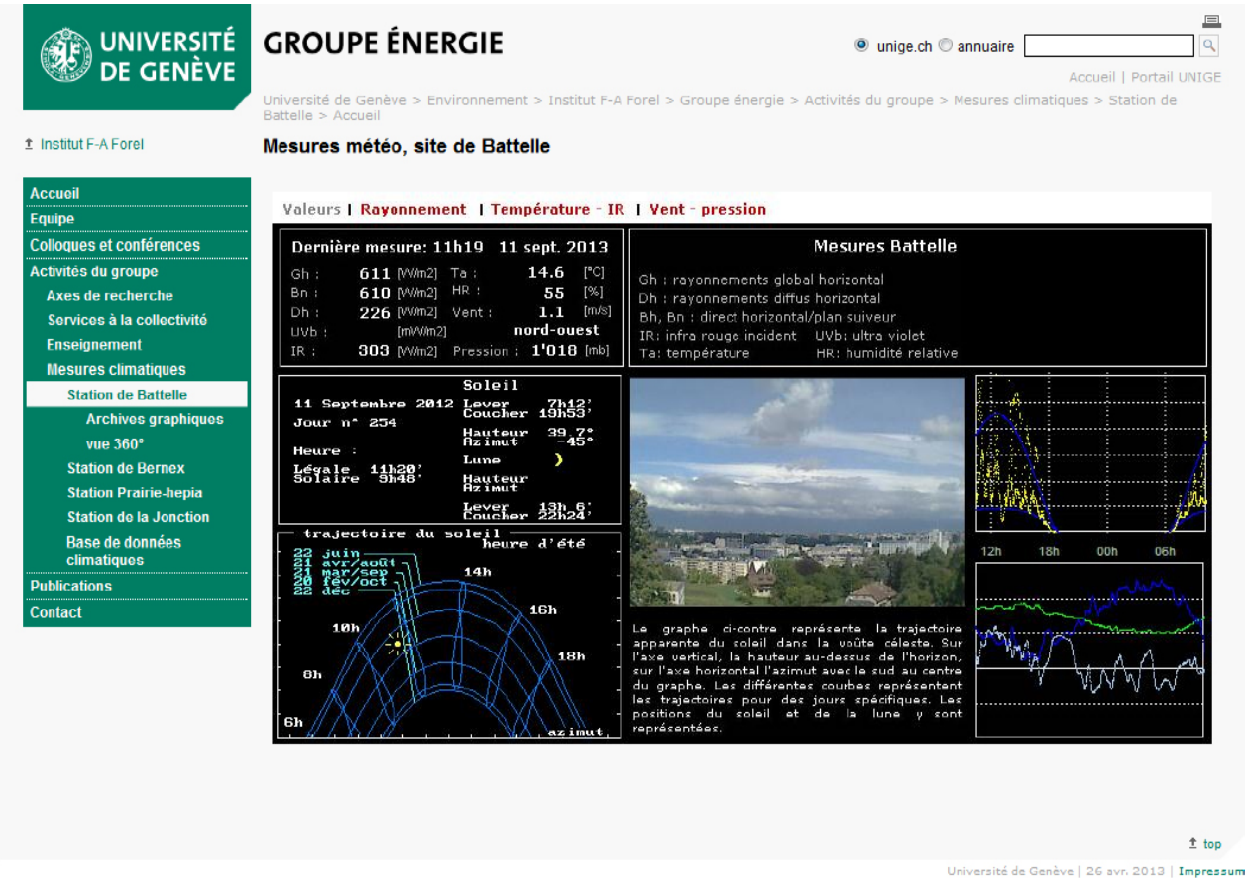

Figure 10 Main windows displaying real time data acquired on the site of Battelle (www.unige.ch/energie/forel/energie/activites/meteo/battelle.html)

Acknowledgements

The solar radiation measurements program in Geneva were financially supported by the Swiss National Fundation for Energy (NEFF), the Ernst and Lucie Schmidheiny Foundation, the Société Académique de Genève, the Geneva's Department of Public Economy and the Federal Office of Energy (OFEN). The ongoing research are financed by the Service Industriels de Genève (SIG) and the Federal Office of Energy (OFEN).

Particular thanks to Pierre Bremer and Antoine Zelenka for their unconditional support at the beginning of our measurements program.

References

Atwater M.A., Ball J.T. (1976) Comparison of radiation computations using observed and estimated precipitable water. J. Appl. Meteorol. 15, 1319-1320.

Baudry F., Ineichen P. (1996). Modélisation de Rayonnement UVB à Genève, University of Geneva

Hoyer-Klick C. et al. (2009) MESoR - Management and exploitation of solar resorce knowledge. In: Solar Paces. Berlin.

Ineichen P. (2006) Comparison of eight clear sky broadband models against 16 independent data banks. In: Solar Energy, vol. 80, n° 4, p. 468-478.

Ineichen P. (2006) Summer climatic data for Geneva: average and extreme conditions. In: PLEA 2006 - The 23rd Conference on Passive and Low Energy Architecture. Geneva.

Ineichen P. (2008) A broadband simplified version of the Solis clear sky model. In: Solar Energy, vol. 82, n° 8, p. 758-762.

Ineichen P. (2008) Comparison and validation of three global-to-beam irradiance models against ground measurements. In: Solar Energy, vol. 82, n° 6, p. 501-512.

Ineichen P. (2008) Conversion function between the Linke turbidity and the atmospheric water vapor and aerosol content. In: Solar Energy, vol. 82, n° 11, p. 1095-1097.

Ineichen P. (2011) Global irradiance on tilted and oriented planes: model validations. University of Geneva. (http://archive-ouverte.unige.ch/unige:23519)

Ineichen P. et al. (1984) Infrared sky radiation in Geneva. In: Solar Energy, vol. 32, n° 4, p. 537-545.

Ineichen P. et al. (1984) Study of the corrective factor involved when measuring the diffuse solar radiation by use of the ring method. In: Solar Energy, vol. 31, n° 1, p. 113-117.

Ineichen P. et al. (1988) Solar radiation transposition models applied to a plane tracking the sun. In: Solar Energy, vol. 41, n° 4, p. 371-377.

Ineichen P. et al. (1990) Ground-reflected radiation and albedo. In: Solar Energy, vol. 44, n° 4, p. 207-214.

Ineichen P. et al. (1994) Sky luminance data validation: Comparison of seven models with four data banks. In: Solar Energy, vol. 52, n° 4, p. 337-346.

Ineichen P. et al. (2000) Modeling direct irradiance from goes visible channel using generalized cloud indices. In: 80th AMS annual meeting. Long beach CA (USA). 2.19 p.

Ineichen P. et al. (2009) Satellite Application Facilities irradiance products: hourly time step comparison and validation over Europe. In: International Journal of Remote Sensing, vol. 30, n° 21, p. 5549-5571.

Ineichen P., Perez R. (1999) Derivation of cloud index from geostationary satellites and application to the production of solar irradiance and daylight illuminance data. In: Theoretical and applied Climatology, vol. 64, n° 1-2, p. 119-130.

Ineichen P., Perez R. (2010) Aerosol quantification based on global irradiance. In: Solar Paces. Perpignan (France).

Ineichen P., Perez, R, Seals, R. (1987) The importance of correct albedo determination for adequately modeling energy received by tilted surfaces. In: Solar Energy, vol. 39, n° 4, p. 301-305.

Ineichen P., Perez, R. (2002) A new airmass independent formulation for the Linke turbidity coefficient. In: Solar Energy, vol. 73, n° 3, p. 151-157.

Kasten F. (1980) A simple parameterization of the pyrheliometric formula for determining the Linke turbidity factor, Meteorol. Rdsch. 33

Meyer R., Gueymard C., Ineichen P. (2011) Standardizing and benchmarking of modeled DNI data products. In: Solar Paces. Perpignan (France).

Michalsky J. et al. (1994) Degradation of solar concentrator performance in the aftermath of Mount Pinatubo. In: Solar Energy, vol. 52, n° 2, p. 205-213.

Molineaux B., Ineichen P. Impact of Pinatubo aerosols on the seasonal trends of global, direct and diffuse irradiance in two northern mid-latitude sites. In: Solar Energy, vol. 58, n° 1-3, p. 91-101.

Molineaux B., Ineichen P. On the broad band transmittance of direct irradiance in a cloudless sky and its application to the parameterization of atmospheric turbidity. In: Solar Energy, vol. 56, n° 6, p. 553-563.

Molineaux B., Ineichen P., Delaunay J.J. Direct luminous efficacy and atmospheric turbidity—Improving model performance. In: Solar Energy, vol. 55, n° 2, p. 125-137.

Molineaux B., Ineichen P., O'Neill N. Equivalence of Pyrheliometric and Monochromatic Aerosol Optical Depths at a Single Key Wavelength. In: Applied Optics, vol. 37, n° 30, p. 7008.

Mueller, R et al. (2004) Rethinking satellite-based solar irradiance modellingThe SOLIS clear-sky module. In: Remote Sensing of Environment, vol. 91, n° 2, p. 160-174.

Perez R., P. Ineichen, E. Maxwell, R. Seals, A. Zelenka (1992) Dynamic global to direct irradiance conversion models. ASHARE Trans. Res. Series, 354-369

Perez, R et al. (1990) Climatic evaluation of models that predict hourly direct irradiance from hourly global irradiance: Prospects for performance improvements. In: Solar Energy, vol. 44, n° 2, p. 99-108.

Perez, R et al. (1990) Making full use of the clearness index for parameterizing hourly insolation conditions. In: Solar Energy, vol. 45, n° 2, p. 111-114.

Perez, R et al. (1990) Modeling daylight availability and irradiance components from direct and global irradiance. In: Solar Energy, vol. 44, n° 5, p. 271-289.

Perez, R et al. (2002) A new operational model for satellite-derived irradiances: description and validation. In: Solar Energy, vol. 73, n° 5, p. 307-317.

Perez, R et al. (2004) Producing satellite-derived irradiances in complex arid terrain. In: Solar Energy, vol. 77, n° 4, p. 367-371.

Perez, R. et al. (1987) A new simplified version of the perez diffuse irradiance model for tilted surfaces. In: Solar Energy, vol. 39, n° 3, p. 221-231.

Perez, R. et al. (1993) Geostatistical properties and modeling of random cloud patterns for real skies. In: Solar Energy, vol. 51, n° 1, p. 7-18.

Suri M. et al. (2009) Comparison of Direct Normal Irradiation Maps for Europe. In: Solar Paces. Berlin.